Received: 29 October 2019 | Accepted: 23 April 2020

DOI: 10.1002/jor.24714

RESEARCH ARTICLE

Journal of Orthopaedic Research®

Moment arm function dictates patella sagittal height anatomy: Rabbit epiphysiodesis model alters limb length ratios and subsequent patellofemoral anatomical development

Michael J. Dan | William C. H. Parr | James D. Crowley | Rema A. Oliver | Kimberley Kai Lun | Vedran Lovric | Mervyn Cross | David Broe | William R. Walsh

Surgical and Orthopaedic Research Laboratories (SORL), Prince of Wales Clinical School, UNSW Sydney, Randwick, New South Wales, Australia

Correspondence
Michael J. Dan, Surgical and Orthopaedic Research Laboratory, Prince of Wales Hospital, Barker St, Randwick, NSW 2052, Australia.
Email: michaeldan@hotmail.com

Abstract

Patellofemoral anatomical dysplasia is associated with patellofemoral instability and pain. The closure of the knee physis occurs at the same age as the peak incidence of patellofemoral dislocation. This study determined the effect on the patellofemoral anatomical development in a rabbit epiphysiodesis model. Twenty-four skeletally immature New Zealand White rabbits were divided into three groups (a) distal femur epiphysiodesis (FE) (b) proximal tibia epiphysiodesis (TE) (c) control; no epiphysiodesis (C) performed at 6 weeks of age. The primary endpoint was shape analysis using three-dimensional reconstructions of micro-computed tomographys (CTs) performed at 30 weeks of age. The limb length ratios (femur:tibia) were significantly different for both FE (mean 0.72, SD 0.0381, $P < .001$) and TE (mean 0.91, SD 0.0383, $P < .001$) treatment groups compared to control (mean 0.81, SD 0.0073). Patella height, as measured from the most distal point of the patella to the tibial joint surface (modified Caton-Deschamps measurement), was lower (baja) in the FE and higher (alta) for the TE, compared with the control group. Our findings suggest femoral and tibial shortening can influence the development of the patellofemoral joint, which may be dictated by moment arm function and is potentially responsible for the etiology of patella alta. Future studies are warranted to explore this association further with the view for the development of treatment options for patella alta in human patients.

KEYWORDS

patella tendinopathy, patellofemoral

1 | INTRODUCTION

Anatomical abnormalities contribute to patellofemoral pain and dislocation, including trochlear dysplasia, excessive distance between tibial tubercle and trochlear groove, and patella alta. Corrective surgical procedures have been proposed to address these predisposing factors in an "a la carte" fashion.[1] It is unknown why different individuals develop these anatomical abnormalities; is it the chicken or the egg, or as phrased by Tanaka "which came first, the patella or the trochlea?".[2] The bi-convex shape of the patella develops in utero

without compression against the femoral trochlea.[3] The femoral trochlea also develops it's characteristic bi-concave shape in utero by 18 weeks,[4,5] suggesting this dysplastic predisposition from birth.

Rabbit research models have been developed to alter the compression of the patella against the trochlea based on previous research on the development and treatment of hip dysplasia in humans.[6] Rabbit models investigating changing patella position through dislocation,[7] reduction or persistent dislocation,[8] subluxation due to medial retinaculum incision[9] or patella alta due to patella tendon lengthening,[10] have all concluded that the less time the patella spends in articulation with the trochlea, the flatter it develops. This finding suggests a developmental contribution to pathological patellofemoral anatomy. In contrast, human studies have suggested that while the magnitude of the trochlea dimensions change with growth, normal trochlea shape[11] or dysplasia[12] is likely genetically predetermined.

This is despite the lack of longitudinal studies in humans investigating patellofemoral anatomical morphology changes with time/growth.

Peak incidence of patellofemoral dislocations occur between the ages of 15 to 19 years,[13,14] which corresponds with closure of the distal femoral and proximal tibial physis.[15] Therefore, the objective of this study was to explore the role of the physis on patellofemoral development. We aimed to determine if isolated epiphysiodesis, to either the distal femoral or proximal tibial physis, altered the tibia to femur limb length ratio and subsequently affected development of the patellofemoral joint in a rabbit model of skeletally immature animals.

2 | MATERIALS AND METHODS

2.1 | Animals

Following approval by the Institutional Animal Care and Ethics Committee (ACEC approval 18/45A, NSW, Australia), 24 6-week-old female New Zealand White rabbits (Biological Research Centre, Sydney, Australia), with a mean weight of 1.2 kg, were equally divided and randomly assigned to one of three groups (a) distal femoral epiphysiodesis (FE) (b) proximal tibial epiphysiodesis (TE), and (c) control; no epiphysiodesis (C). All rabbits were systemically well with a normal body condition and no orthopedic or neurological abnormalities based on examination by a veterinarian (JC). The rabbits were acclimatized for 1 week with a maximum of four rabbits per pen, housed at 22°C with a 12-hour day-night cycle. The rabbits were maintained on timothy hay straw and commercial pellets (Gordan's Specialty Stockfeeds, NSW, Australia), supplemented with fresh dark leafy greens and other vegetables. Water was provided ad libitum.

2.2 | Anesthesia and perioperative care

The rabbits were premedicated with buprenorphine (0.03 mg/kg) and midazolam (0.5 mg/kg) via intramuscular injection using a 26 g insulin needle. The rabbits were preoxygenated for 10 minutes prior to masked isoflurane induction and maintained between 2% and 3%, titrated to effect. Continuous multiparameter cardiopulmonary monitoring (Datalys V7; Lutech, Ronkonkoma, NY) was used throughout anesthesia. The rabbits received external heat support in the form of a heat pad. Following completion of surgery, the rabbits were wrapped in a towel for added warmth and received masked oxygen supplementation until righting before being returned to their housing pen. Prophylactic antibiotics (Enrofloxacin 5 mg/kg IM) was provided prior to surgery and continued for 5 days postoperatively. Carprofen (2 mg/kg s/c) was administered for postoperative analgesia and inflammation. Buprenorphine (0.02-0.05 mg/kg IM) was administered for rescue analgesia as indicated. The rabbits were monitored daily for the first week postoperative, paying particular attention to appetite, demeanor, the surgical site and requirement for additional analgesia. The rabbits were weighed weekly prior to euthanasia at 6 weeks postoperative (30 weeks old) via intracardiac pentobarbitone injection under general anesthesia.

2.3 | Surgery

All surgical procedures were completed by a senior orthopaedic registrar (MD) and veterinary surgeon (JC). For all treatment groups, both hindlimbs were clipped from the proximal femoral region to the tarsus and aseptically prepared for surgery (povidine-iodine solution). The medial stifle was aseptically draped into the sterile field using disposable, impermeable drapes. A medial skin incision (~3-5 cm) was made from the parapatellar region to 1 cm distal to the tibial crest. The same skin incision was performed for all animals, regardless of the treatment group. The physis of interest was approached via a combination of blunt and sharp dissection and located via placement of a 23 g sterile needle, confirmed via a portable fluoroscopy unit (Shanghai Bojin Electric Instrument & Device Co, Shanghai, China). The periosteum overlying the physis was sharply incised prior to physical and heat ablation using a high-speed motorized burr (Midas Rex, Medtronic, Memphis, TN), as previously described.[1,16] Briefly, the burr was directed perpendicular to the physis and burring performed under high speed in all directions along entire length of the physis using a fanning motion. To serve as future radiographic reference points, a 0.6 mm Kirschner wire was cut into 1 to 2 mm lengths and inserted parallel to the physis in the adjacent distal femur and proximal tibial metaphysis in a mediolateral direction for all treatment groups. The Kirschner wire lengths penetrated the near (cis) cortex only. Fascial and subcutaneous tissues were closed in a simple continuous pattern (3-0 Vicryl). The skin was closed with intradermal sutures (3-0 Vicryl). All rabbits recovered uneventfully from surgery and were returned to their housing pen with no exercise restrictions placed on them for the duration of the study.

2.4 | Diagnostic imaging

Bilateral orthogonal hindlimb radiographs (anterior-posterior and mediolateral) were performed at 0, 3, 6 and 24 weeks postoperatively

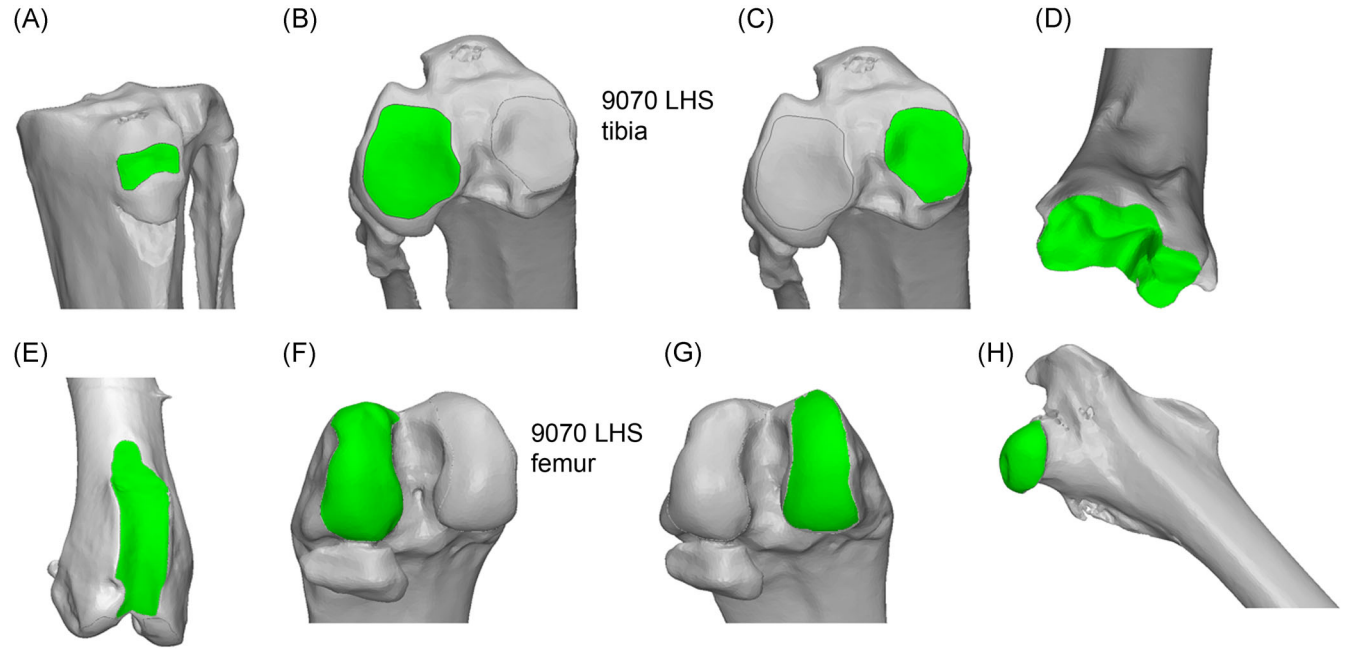

FIGURE 1 Isolated tibial (above) and femoral (below) articular surfaces. A, tibial tuberosity, B, lateral proximal tibia, C, medial proximal tibia, D, distal tibia (talocrural), E, femoral trochlea, F, medial femoral condyle, H, lateral femoral condyle and I) femoral head [Color figure can be viewed at wileyonlinelibrary.com]

under general anesthesia using the previously described anesthetic protocol. Radiographs were processed by a Faxitron (Faxitron Bioptics, LLC, Arizona) and digital plates (AGFA CR MD4.0 Cassette, AGFA, Germany) at 24 kV over 45 seconds. An AGFA Digital Developer and dedicated workstation was used to process the digital images (AGFA CR 75.0 Digitizer Musica, AGFA, Germany). The DICOM data was converted to Bitmap images using DICOM Works (ez-DICOM medical viewer, copyright 2002). Physeal closure and Kirschner wire positioning were evaluated on all acquired radiographs by two blinded observers.

All rabbits underwent helical multidetector micro-computed tomographic (micro-CT) evaluation (resultant slice thickness of 120 μm) of both hindlimbs at 24 weeks postoperative following euthanasia (MILabs, Utrecht, the Netherlands). The knee was maintained at 30° of flexion for all acquired images, to maintain patella tendon tension.

2.5 | Three-dimensional reconstruction—segmentation of micro-CT images

Three-dimensional (3D) isosurface boundary representations (b-reps) of the right and left hindlimbs were reconstructed from micro-CT DICOM images using Materialize MIMICS vs 19 (Leuven, Belgium). Models were femora, tibia, and patellae from the right hand side (RHS) and left hand side (LHS) hindlimbs were separated during the segmentation process. Following 3D reconstruction, tibial, femoral and patella articular surfaces were isolated to enable subsequent analysis (Figure 1). Note that the articular surfaces were maintained in the same position relative to one another.

2.6 | Morphological analyses—femoral coordinate system

Spheres and planes were fitted to the articular surfaces identified above using least-squares minimization. The coordinate system was adapted from the International Society of Biomechanics (ISB) recommendations.[17] Differing from ISB recommendations,[17] 0,0,0 for the coordinate system was set at the centroid of the distal tibial articular surface. The centre of rotation of the hip joint was calculated as the centre point of a sphere fitted to the articular surface of the femoral head (Figure 2) and was used to define the orientation (main axis) of the femoral coordinate system.

In contrast to Wu et al,[17] spheres were also fitted to the medial and lateral femoral condyles as described previously.[18,19] Fitting spheres to the femoral condyles should reduce intra- and inter-user error in defining femoral epicondyles.[17] The midpoint of the line between the centres of these two spheres was defined (Figure 3); akin to the midpoint of the femoral epicondyles as described by Wu et al.[17]

The *y*-axis was defined as the vector between the midpoint between the femoral condyle fitted spheres and the centre of rotation for the femoral head articular surface. The *x*-axis was defined as the cross product of the *y*-axis vector and the vector between the centres of the spheres fitted to the medial and lateral femoral condyles. The axes were set so that anterior orientation represented a positive value. The *z*-axis was defined by taking the cross product of the *y* and *x* axes and set so that lateral was positive. Once the coordinate system was defined, each specimen was moved so that the centroid of the tibial talocrural joint surface was at 0,0,0 and rotated so

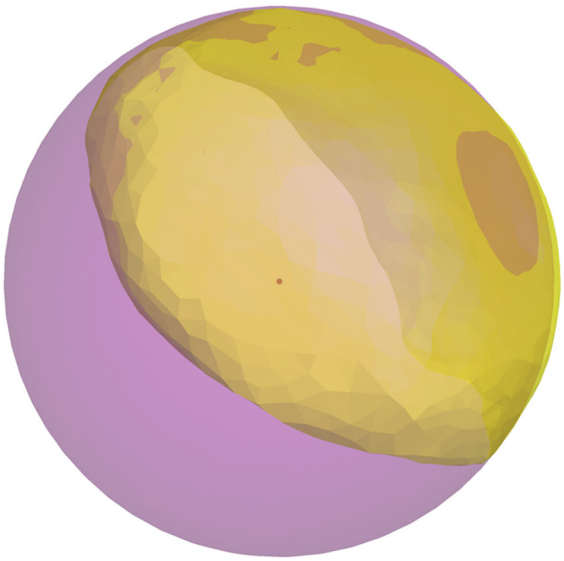

FIGURE 2 Sphere (purple) fitted to the articular surface (yellow) of the RHS femoral head. The calculated centre point of the fitted sphere is shown [Color figure can be viewed at wileyonlinelibrary.com]

that the femoral coordinate system was aligned with the global coordinate system (Figure 4). Femur lengths were calculated as the length of the vector from the centre of the sphere fitted to the femoral head articular surface to the mid-point between the sphere centre points fitted to the medial and lateral femoral condyles. Tibial lengths were calculated as the mid-point between the two centroids of the proximal tibial articular surfaces (medial and lateral) and the centroid of the distal (talocrural) articular surface.

Femoral trochlea articular glide length was defined as the arc length of a sphere fitted to the femoral trochlea articular surface (Figure 5).

Sagittal patella sphere radius, articular glide length and theta were also calculated for the patella using a similar method (Figure 6). As the trochlea and patella articular surfaces are curved in two planes (longitudinal and transverse), central strips of these facets were isolated and fitted with 2D (Figure 5) and 3D (Figure 6) circles/spheres to capture the longitudinal curvature (the major axis curvature) for analysis. Using the central strip allows identification of the centre point of rotation during knee flexion and extension, whereas the transverse curvature (trochlea groove depth) is associated with maintaining the patella in the trochlea groove, thereby preventing dislocation during flexion and extension movements. The goodness of fit of this method is depicted in Figures 5 and 6.

To assess the extents of the influence of function (the need to articulate with, and slide across the femoral trochlea articular surface) on the anatomy of the patella articular surface curvature, the centre points of rotation for the patella and femoral trochlea articular surfaces were calculated. If the only constraint on the patella morphology was to fit with and move across the trochlea, it could be expected that the centre points of spheres fitted to the major axis curvature of both articular surfaces would be coincidental.

To further assess patella height positioning between treatment groups, distances between the patella and the previously defined distal femoral and proximal tibial articular surfaces were calculated (Figure 7). We related these measurements to clinically used measurements reflecting the Caton-Deschamps index,[20] Insall-Salvati ratio[21] was taken as the distance between the centre of the tibial patella tendon insertion (red) and the centre of the patella articular surface (solid black line). The patella-trochlea engagement measurement[22] was defined as the distance between the centre of the patella articular surface and the most superior point of the femoral trochlea articular surface (dashed line). The patella tendon length (dot-dashed black line) was measured from the inferior pole of the patella to the centre of the patella tendon insertion on the tibia (red).

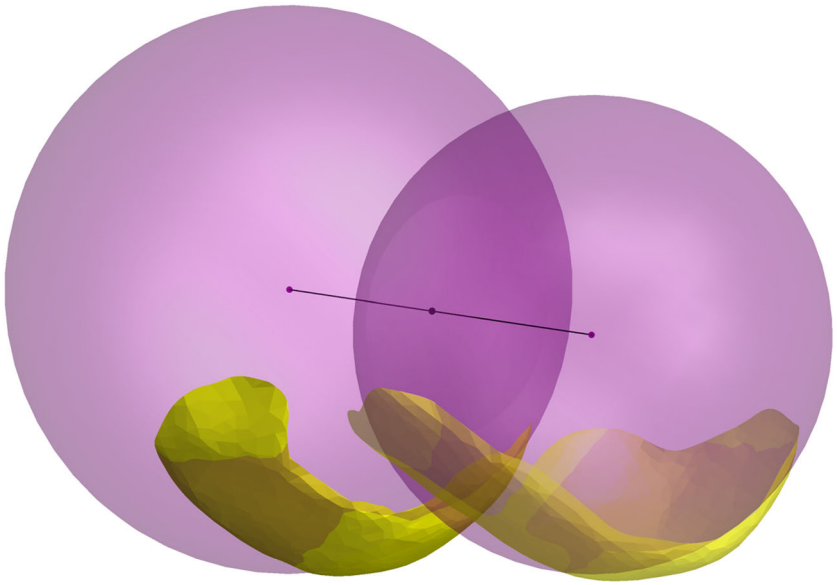

FIGURE 3 Spheres (purple) fitted to the medial and lateral femoral condyles (yellow) of the right hindlimb. The medial epicondyle is on the right-hand side of the figure and the lateral epicondyle is on the left-hand side of the figure [Color figure can be viewed at wileyonlinelibrary.com]

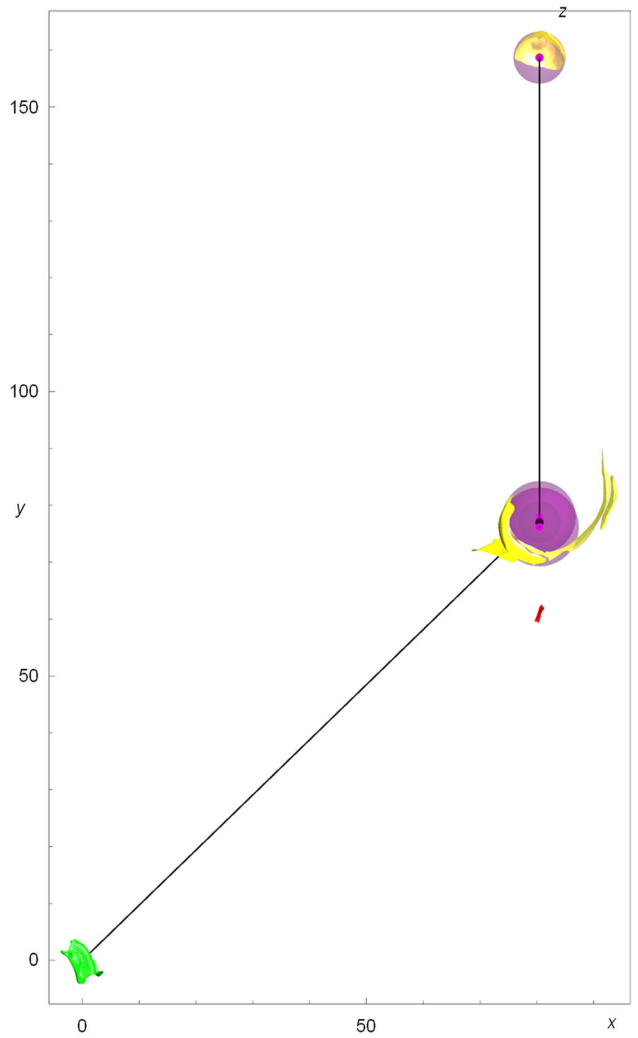

FIGURE 4 Selected articular surfaces for the left hindlimb oriented within the global coordinate system. The black lines represent the tibial and femoral lengths. The angle between the black lines in the xy plane was taken as the flexion angle. The angle between the black lines in the zy plane was taken as the varus-valgus angle. The *y*-axis represents the vertical axis. The *x*-axis represents the horizontal axis [Color figure can be viewed at wileyonlinelibrary.com]

The medial and lateral aspects of the patella articular surface were partitioned using a modified watershed algorithm (Figure 8A). Planes were fitted to the medial and lateral aspects of the patella surface and the angle between the normal vectors of these two planes was calculated (Figure 8B).

2.7 | Statistical analysis

Quantitative parameters between treatment groups were analysed by analysis of variance. A post hoc Tukey's HSD multiple comparison test was used to detect significant differences between the treatment effects. For nonnormally distributed data, nonparametric Kruskal-Wallis tests were used to compare the treatment effects. Significance was set at an α level of $P < .05$. All data is presented as the mean and the standard deviation of the mean. Reliability was tested with the intraclass correlation coefficient (ICC) via a two-way mixed model. Analysis was performed using SPSS version 18.0 for Windows (SPSS Inc, Chicago, IL).

3 | RESULTS

Descriptive statistics for post hoc Tukey's HSD multiple comparison tests are presented in Table 1.

3.1 | Radiographs

For all rabbits in groups FE and TE, postoperative radiographs demonstrated successful cessation of growth by the lack of change in the distance between the Kirschner wires and the adjacent ablated physis compared with the continued growth away from the unaffected physis respectively. No other radiographic abnormalities such as fractures and subluxations were noted for any animal at all radiographic time points.

3.2 | Limb length ratios

The limb length ratios (femur:tibia) were significantly different for both group FE (mean 0.72, SD 0.04, $P < .001$) and group TE (mean 0.91, SD 0.04, $P < 0.001$) compared with group C (mean 0.81, SD 0.01) (Figure 9).

3.3 | Patellar height

Patella height, as measured from the most distal point of the patella to the tibial joint surface (modified Caton-Deschamps index), was lower (baja) in group FE and higher (alta) for group TE, compared to the group C (Figure 9).

The limb length ratio was correlated with the tibial joint surface to patella height measurement (modified Caton-Deschamps index; ICC = 0.63, $P = .01$). The patella tendon length was correlated to the modified Insall-Salvati index (ICC 0.92, $P = .01$), while the limb length ratio to Insall-Salvati index was not (ICC 0.25). This is reflected by group FE having a significantly shorter patellar tendon length ($P = .01$) and shorter Insall-Salvati index ($P = .04$), compared with group C. There was no significant difference between groups C and TE for patellar tendon length ($P = .15$) and Insall-Salvati index ($P = .75$).

3.4 | Trochlea curve

The trochlea sphere radius was smaller in group FE (mean 14.08 mm, SD 3.83 mm) compared with group C (mean 14.82 mm, SD 1.72 mm),

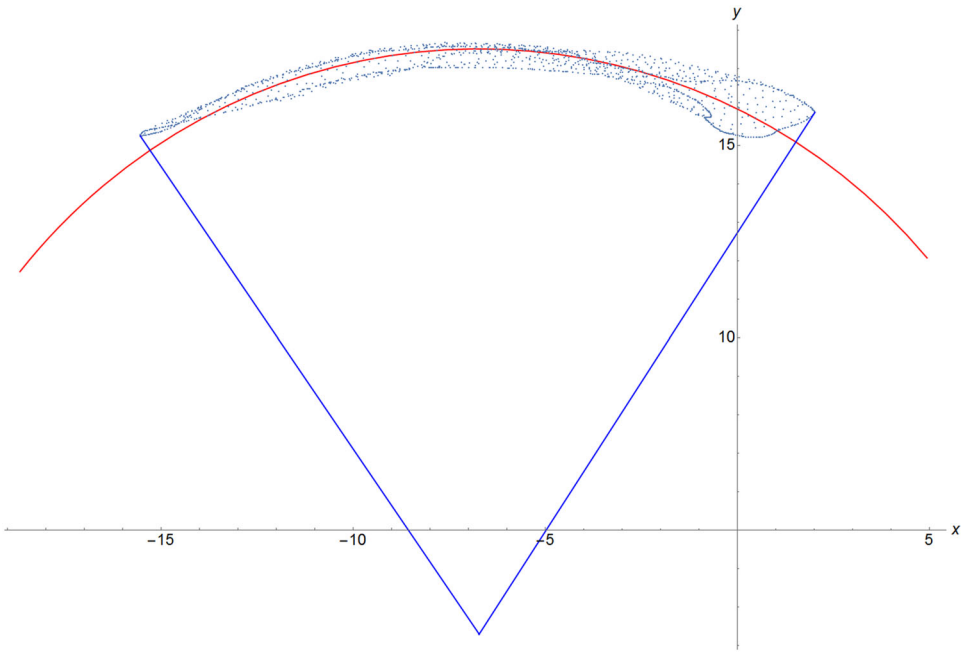

FIGURE 5 Two-dimensional (2D) representation of the calculation of the femoral trochlea articular surface glide length. Arc length (red) was defined by vectors (blue) from the fitted sphere centre point to the extents of the aligned articular surface. Theta was calculated as the angle between the two extent vectors [Color figure can be viewed at wileyonlinelibrary.com]

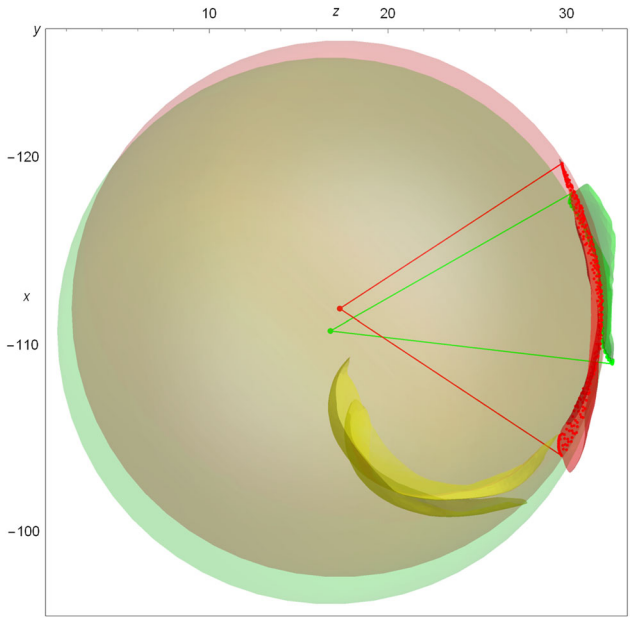

FIGURE 6 Fitted spheres for the patella and distal femoral condyles (yellow) in the mediolateral (xy) plane. Spheres were fitted to the central strip of the left patella (green) and femoral trochlea (red). The red lines define the extent of the arc length, with the resultant angle between the lines defined as theta. The defined points represent the centre point of the spheres fitted to the articular surfaces. The y-axis represents the vertical axis, with the x-axis representing the horizontal axis of the coordinate system as defined [Color figure can be viewed at wileyonlinelibrary.com]

however, was not statistically significant ($P = .74$). The trochlea sphere radius for group TE (mean 15.22 mm, SD 2.15 mm) was greater than group C but was not statistically significant ($P = .92$).

Femoral trochlea length for group FE was significantly shorter than group C ($P = .01$), however, there was no significant difference between group C and group TE ($P = .94$). Femoral trochlea theta for group FE (74.71°, SD = 21.11) was significantly smaller than group C (89.44°, SD = 8.18, $P = .03$), however, there was no significant difference between group C and TE ($P = .72$).

For group FE, the difference in the trochlea and patella centre point of rotation (mean, SD was significantly shorter than the TE ($P < .001$) and control group ($P = .002$), however, there was no statistical difference between TE and C ($P = .91$).

3.5 | Patella

Patella length ($P = .58$), angle between medial and lateral articular surfaces ($P = .77$), and sagittal radius of curvature ($P = .14$) did not differ between treatment groups. Trochlea sphere ratio was correlated to the patellar sphere ratio (ICC 0.60, $P = .05$).

4 | DISCUSSION

This study demonstrates that distal femoral and proximal tibial epiphysiodesis alters the limb length ratios and subsequent patellar height in a skeletally immature rabbit cohort. Compared with the control group, relative patella baja and a shorter femur (group FE)

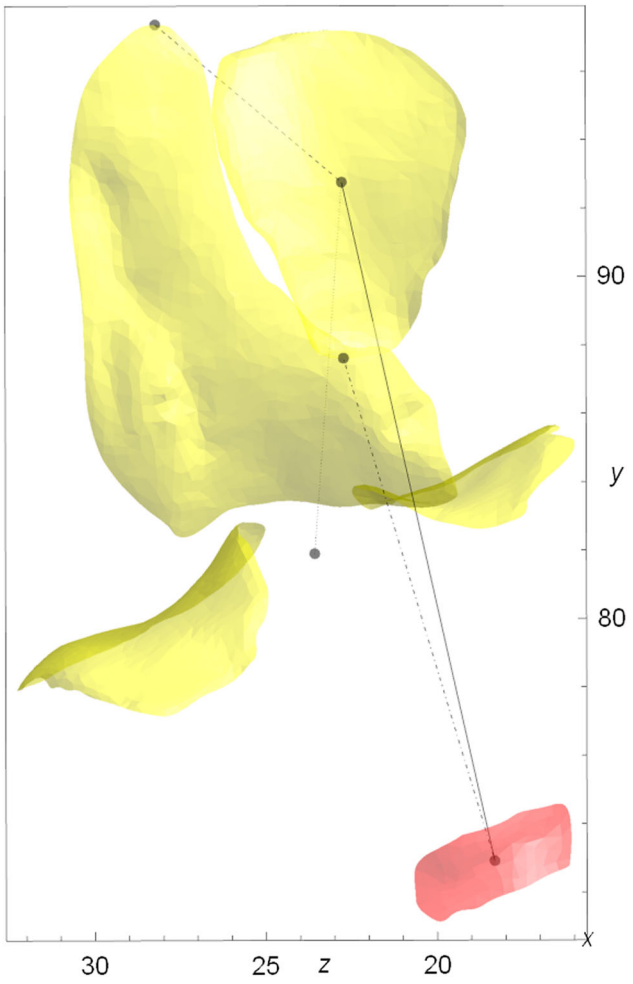

FIGURE 7 Articular surfaces for the trochlea, patella, medial and lateral tibial plateaus in the anterior (yz) plane. The Caton-Deschamps measurement for patella height was taken as the distance between the midpoint of the tibial plateau to the inferior pole of the patella. The Insall-Salvati measurement was taken as the distance between the centre of the tibial patella tendon insertion (red) and the centre of the patella articular surface (solid black line). The patella- trochlea engagement measurement was defined as the distance between the centre of the patella articular surface and most superior point of the femoral trochlea articular surface (dashed line). The patella tendon length (dot-dashed black line) was measured as the inferior pole of the patella to the centre of the patella tendon insertion on the tibia (red) [Color figure can be viewed at wileyonlinelibrary.com]

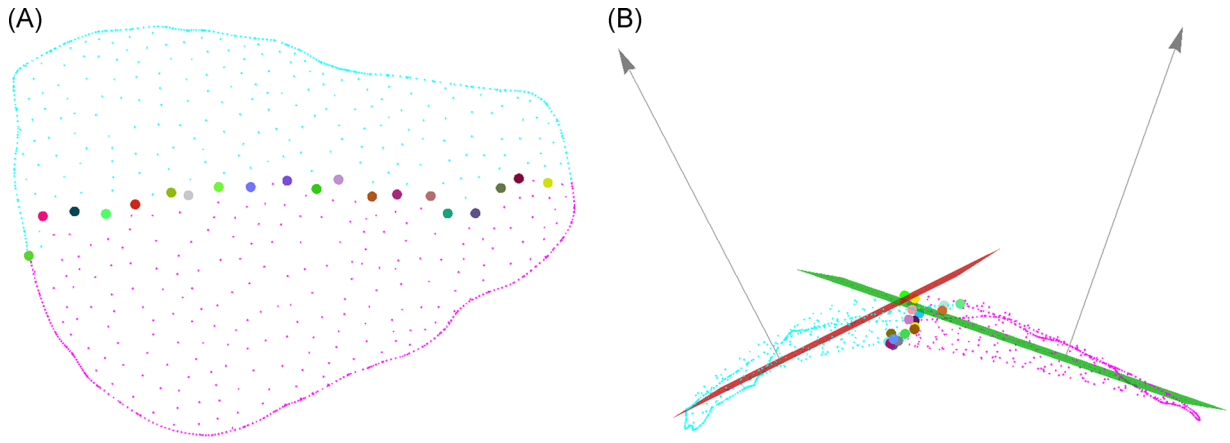

FIGURE 8 A, Separation of medial and lateral aspects of the patella articular surface using a modified watershed algorithm (watershed line shown by larger points). B, Medial (red) and lateral (green) planes were fitted to the respective aspects of the patella articular surface. Normal vectors for these respective planes are represented by the gray arrows [Color figure can be viewed at wileyonlinelibrary.com]

TABLE 1 Descriptive statistics for post hoc Tukey's HSD multiple comparison tests for multiple parameters between treatment groups

	Treatment group				
	Control (C)	Femoral epiphysiodesis (FE)		Tibial epiphysiodesis (TE)	
	Mean (SD)	Mean (SD)	*P* value	Mean (SD)	*P* value
Femur length (mm)	85.51 (3.03)	75.65 (4.48)	**<.001**[a]	86.04 (2.82)	.91[a] **<.001**[b]
Tibia length (mm)	105.02 (3.78)	104.88 (2.39)	.99[a]	94.49 (4.13)	**<.001**[a] <**.001**[b]
Limb length (femur:tibia) ratio	0.81 (0.01)	0.72 (0.04)	**<.001**[a]	0.91 (0.04)	**<.001**[a] <**.001**[b]
Patellar tendon length (mm)	19.36 (0.96)	17.31 (1.79)	**.001**[a]	18.36 (1.40)	.15[a] .11[b]
	9.43 (2.84)	3.17 (4.66)	**<.001**[a]	6.00 (4.31)	.06[a] .13[b]
Insall-Salvati Index	20.13 (2.04)	18.07 (2.79)	**.001**[a]	19.53 (1.73)	**.06**[a] .18[b]
Modified Caton-Deschamps Index	20.87 (1.76)	18.89 (1.06)	**.04**[a]	22.81 (2.18)	**.02**[a] <**.001**[b]
Patella to femoral trochlea distance	9.64 (2.73)	7.45 (2.19)	.10[a]	7.33 (3.52)	.08[a] .99[b]
Angle between medial/lateral articular surfaces	53.40 (5.43)	51.88 (10.08)	.85[a]	51.42 (6.52)	.76[a] .99[b]
Sagittal patella articular glide length	9.35 (0.55)	9.24 (0.89)	.90[a]	9.50 (0.61)	.84[a] .56[b]
Patella theta	8.18 (2.19)	21.11 (5.28)	.15[a]	12.69 (3.17)	.52[a] .69[b]
Sagittal patella sphere radius	10.69 (1.16)	13.19 (5.86)	.16[a]	11.13 (1.44)	.94[a] .25[b]
Femoral trochlea articular glide length	21.48 (2.18)	16.47 (3.13)	**<.001**[a]	21.26 (4.02)	.98[a] <.001[b]
Femoral trochlea theta	89.44 (8.18)	74.71 (21.11)	**.030**[a]	85.13 (12.69)	.721[a] .141[b]
Trochlea sphere radius	14.82 (1.72)	14.08 (3.83)	.742[a]	15.22 (2.15)	.920[a] .479[b]
Difference in the trochlea and patella centre point of rotation	4.98 (2.21)	0.68 (3.50)	**.002**[a]	5.47 (3.67)	.91[a] **<.001**[b]
Knee flexion angle	44.38 (13.72)	45.06 (11.48)	.99[a]	34.09 (15.06)	.11[a] .07[b]

Note: Significant values are highlighted in bold.
[a]Compared to group C.
[b]Compared to group FE.

and relative patella alta and a shorter tibia (group TE), was induced by epiphysiodesis.

In evolutionary science, it is widely accepted that function dictates anatomy.[23] The function of the patella is to (a) decrease the coefficient of friction between the extensor mechanism and the trochlea,[24] (b) act as a lever to alter the relative quadriceps tendon to patellar tendon force ratio with changing degrees of knee flexion,[25] and (c) increase the moment arm of the knee.[26] Patella alta is associated with decreased joint contact area,[27] subsequent increased patellofemoral contact forces[28] and the development of patellofemoral arthritis.[29] Patella alta is also widely recognized to increase the efficacy of the extensor mechanism due to the greater

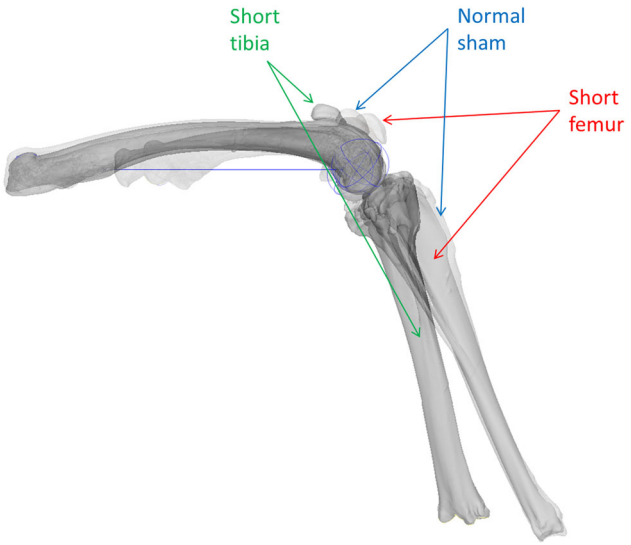

FIGURE 9 3D model representation of limb length ratios and modified Caton-Deschamps measurements for groups C, FE and TE. 3D, three-dimensional; Group FE: relatively short femur/long tibia with patellar baja; Group TE, relatively long femur/short tibia with patellar alta [Color figure can be viewed at wileyonlinelibrary.com]

moment arm of the patella in knee extension compared with knee flexion.[30]

In our study, distal femoral and proximal tibial epiphysiodesis changed the relative limb length ratio and therefore, the relative sagittal balance of the hindlimb. There is an increased distance from the knee to bodyweight axis with a longer femur (tibial epiphysiodesis) and a decreased distance from the knee to the bodyweight axis with a short femur (femoral epiphysiodesis). Given that the torque on either side of the knee needs to balance for a joint to be in equilibrium, if the distance from the knee to the axis of the bodyweight is increased, the force required to balance this torque at the knee is also increased. If the muscular force generated is constant, the only way to increase the torque of the extensor mechanism is to increase the moment arm. The moment arm function of the patella seems to dictate the sagittal patellofemoral anatomical height; however, given we could not precisely control knee flexion angle, we were unable to confirm this by measuring the distance between the patella and femoral epicondyles, as with increasing knee flexion there is increased patella engagement within the trochlea/translation distally which will affect this measurement. Therefore we make the inference from the work of Ward et al[30] where patella alta has been shown to increase the moment arm and extensor mechanism efficacy.

Patella height and trochlea curve are interrelated.[31] In our study, we demonstrated that the sagittal curvature of the patella height was related to the trochlea's radius of curvature. As patella height increased, a shorter, more curved trochlea developed. This finding suggests that the patella's maximal moment arm associated with knee extension is maintained for longer in moving from extension to flexion before the necessary trochlea depth relative to the condyles develops to allow for terminal knee flexion with a relatively longer femur (Figure 10). Additionally, given that the distal femoral physis

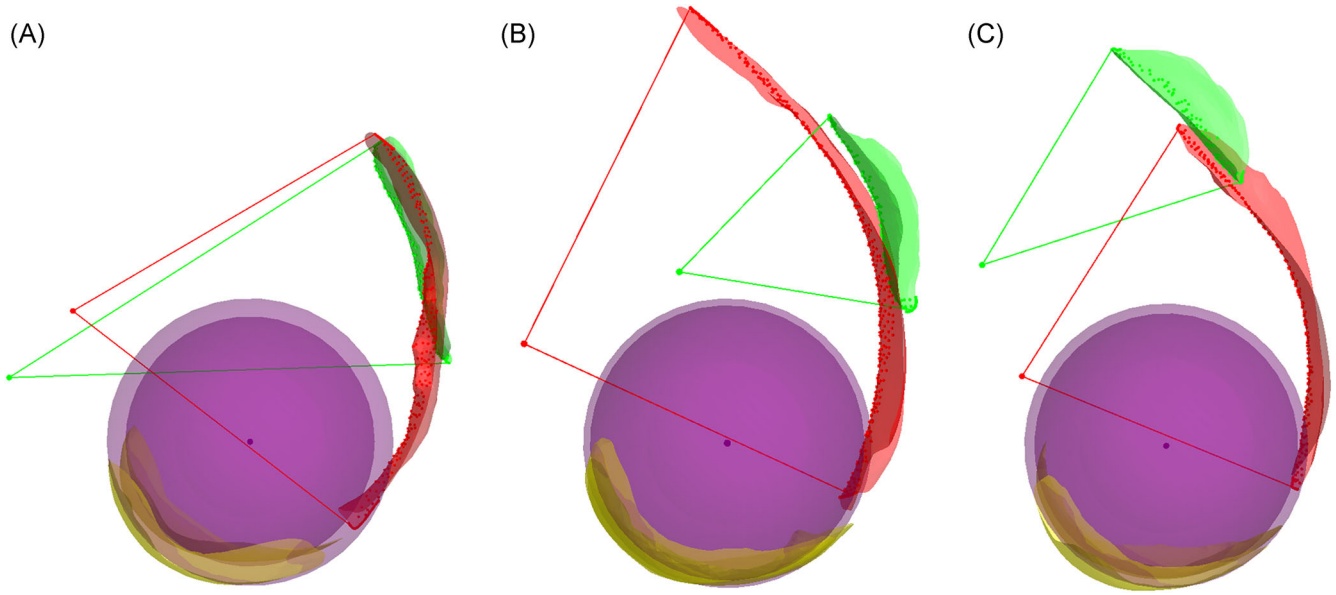

FIGURE 10 A, Femoral epiphysiodesis (FE), B, control (C), and C, tibial epiphysiodesis (TE) treatment group representative samples. Femoral condyles (yellow), fitted spheres (purple, centre of rotation shown by the dark purple point in the spheres), femoral trochlea (red) and patella (green) are shown for all treatment groups. Viewpoints are aligned with the calculated femoral condyle axis of rotation (defined by the vector between medial and lateral condyle fitted sphere centre points). A, Group FE: shorter trochlea, less curved than B the Control group, centre point of rotation for the femoral trochlea surface closer to the patella compared to B control group. B, Control Group: The patella radius of curvature is less than the femoral trochlea radius of curvature. Centre points of rotation for the patella and trochlea surfaces are not coincidental, nor close to one another. C, Group TE: Larger radius of curvature and shorter trochlea than B group C [Color figure can be viewed at wileyonlinelibrary.com]

contributes directly to trochlear development,[12] a shallow trochlear depth may be explained by distal femoral physeal closure.

Limb length ratios are meant to be constant; a tibia to femur ratio of 0.8.[32] Human cadaveric data suggests that increasing this ratio (longer tibia) predisposes an individual to hip and knee arthritis.[33] The clinical relevance of altered limb length ratios is otherwise largely not appreciated. This study opens pandoras box to investigate the association between limb length ratios and patellar height and subsequent dislocation in humans. Longitudinal studies are indicated to determine if patella alta is associated with premature physeal closure and/or a developmental response to a weaker quadriceps mechanism. Additionally, potential early surgical interventions for skeletally immature patients with patellar alta and trochlea dysplasia requires further study.

Our study was limited given we were unable to perform shape analysis to reflect trochlea dysplasia; however, this has been well documented in previous human and animal-based studies.[7,12] The role of the anterior femoral physis in the development of trochlear dysplasia has been previously explored.[12] It was outside the scope of our study to investigate this; however, further investigation is warranted to explore the value of selective femoral epiphysiodesis in the treatment of trochlea dysplasia for skeletally immature patients.[12] The tibial apophysis was also not ablated in our study and therefore, the effect of tibial apophyseal closure on patellar height could not be assessed.

5 | CONCLUSION

Distal femoral and proximal tibial epiphysiodesis altered the relative limb length ratio of the hindlimb in this experimental rabbit model. The associated limb length ratios lead to developmental differences in patellar height with associated morphological changes to the curvature of the trochlea whilst patella morphology remained unchanged. Our findings suggest anatomical development of the patellofemoral joint is dictated by moment arm function and is potentially responsible for the etiology of patella alta. Future studies are warranted to explore this association further with the view for the development of treatment options for patella alta in human patients.

ACKNOWLEDGMENTS

All authors have no conflict of interest. All authors do not have any interest or relationship, financial or otherwise, that might be perceived as influencing an author's objectivity.

AUTHOR CONTRIBUTIONS

All authors have made substantial contributions to research design, or the acquisition, analysis or interpretation of data; drafting the paper or revising it critically; approval of the submitted and final versions. All authors have read and approved the final submitted manuscript.

ORCID

Michael J. Dan http://orcid.org/0000-0002-3193-8048
Rema A. Oliver http://orcid.org/0000-0002-2381-7326
William R. Walsh http://orcid.org/0000-0002-5023-6148

REFERENCES

1. Hall-Craggs ECB. The effect of experimental epiphysiodesis on growth in length of the rabbit's tibia. *J Bone Joint Surg Br*. 1968;50(2):392-400.
2. Tanaka MJ. Editorial commentary: which came first, the patella or the trochlea? Morphological relationships in patients with patellar instability. *Arthroscopy*. 2018;34(6):1929-1930.
3. Vries B. Zur Anatomie der Patella. Vehr. Anat. *Ges Anat An., Ergänzungsh Z Bd*. 1908;32:163-169.
4. Gray D, Gardner E. Prenatal development of the human knee and superior tibiofibular joints. *Am J Anat*. 1950;86(2):235-287.
5. Doskocil M. Formation of the femoropatellar part of the human knee joint. *Folia Morphol*. 1985;33(1):38-47.
6. Weinstein SL. Natural history of congenital hip dislocation (CDH) and hip dysplasia. *Clin Orthop Relat Res*. 1987;225:62-76.
7. Li W, Wang Q, Wang F, Zhang Y, Ma L, Dong J. Femoral trochlear dysplasia after patellar dislocation in rabbits. *Knee*. 2013;20(6):485-489.
8. Wang S, Ji G, Yang X, et al. Femoral trochlear groove development after patellar subluxation and early reduction in growing rabbits. *Knee Surg Sports Traumatol Arthrosc*. 2016;24(1):247-253.
9. Huri G, Atay OA, Ergen B, Atesok K, Johnson DL, Doral MN. Development of femoral trochlear groove in growing rabbit after patellar instability. *Knee Surg Sports Traumatol Arthrosc*. 2012;20(2):232-238.
10. Kaymaz B, Atay OA, Ergen FB, et al. Development of the femoral trochlear groove in rabbits with patellar malposition. *Knee Surg Sports Traumatol Arthrosc*. 2013;21(8):1841-1848.
11. Nietosvaara Y. The femoral sulcus in children. An ultrasonographic study. *J Bone Joint Surg Br*. 1994;76(5):807-809.
12. Parikh SN, Rajdev N, Sun Q. The growth of trochlear dysplasia during adolescence. *J Pediatr Orthop*. 2018;38(6):e318-e324.
13. Waterman BR, Belmont PJ, Owens BD. Patellar dislocation in the United States: role of sex, age, race, and athletic participation. *J Knee Surg*. 2012;25(01):051-058.
14. Sanders TL, Pareek A, Hewett TE, Stuart MJ, Dahm DL, Krych AJ. Incidence of first-time lateral patellar dislocation: a 21-year population-based study. *Sports Health*. 2018;10(2):146-151.
15. Harcke HT, Synder M, Caro PA, Bowen JR. Growth plate of the normal knee: evaluation with MR imaging. *Radiology*. 1992;183(1):119-123.
16. Hall-Craggs EC, Lawrence CA. The effect of epiphysial stapling on growth in length of the rabbits tibia and femur. *J Bone Joint Surg Br*. 1969;51(2):359-365.
17. Wu G, Siegler S, Allard P, et al. ISB recommendation on definitions of joint coordinate system of various joints for the reporting of human joint motion—part I: ankle, hip, and spine. *J Biomech*. 2002;35(4):543-548.
18. Parr WCH, Chatterjee HJ, Soligo C. Calculating the axes of rotation for the subtalar and talocrural joints using 3D bone reconstructions. *J Biomech*. 2012;45(6):1103-1107.
19. Parr WCH, Soligo C, Smaers J, et al. Three-dimensional shape variation of talar surface morphology in hominoid primates. *J Anat*. 2014;225(1):42-59.
20. Caton J, Deschamps G, Chambat P, Lerat JL, Dejour H. [Patella infera. Apropos of 128 cases]. *Rev Chir Orthop Reparatrice Appar Mot*. 1982;68(5):317-325.
21. Insall J, Salvati E. Patella position in the normal knee joint. *Radiology*. 1971;101(1):101-104.

22. Dejour D, Ferrua P, Ntagiopoulos PG, et al. The introduction of a new MRI index to evaluate sagittal patellofemoral engagement. *Orthop Traumatol Surg Res*. 2013;99(8 Suppl):S391-S398.
23. Moss ML, Young RW. A functional approach to craniology. *Am J Phys Anthropol*. 1960;18(4):281-292.
24. Hungerford DS, Barry M. Biomechanics of the patellofemoral joint. *Clin Orthop Relat Res*. 1979;144:9-15.
25. Huberti HH, Hayes WC, Stone JL, Shybut GT. Force ratios in the quadriceps tendon and ligamentum patellae. *J Orthop Res*. 1984;2(1):49-54.
26. Kaufer H. Mechanical function of the patella. *J Bone Joint Surg Am*. 1971;53(8):1551-1560.
27. Ward SR, Terk MR, Powers CM. Patella alta: association with patellofemoral alignment and changes in contact area during weight-bearing. *J Bone Joint Surg Am*. 2007;89(8):1749-1755.
28. Ward SR, Powers CM. The influence of patella alta on patellofemoral joint stress during normal and fast walking. *Clin Biomech*. 2004;19(10):1040-1047.
29. Stefanik JJ, Zhu Y, Zumwalt AC, et al. Association between patella alta and the prevalence and worsening of structural features of patellofemoral joint osteoarthritis: the multicenter osteoarthritis study. *Arthritis Care Res*. 2010;62(9):1258-1265.
30. Ward SR, Terk MR, Powers CM. Influence of patella alta on knee extensor mechanics. *J Biomech*. 2005;38(12):2415-2422.
31. Ferlic PW, Runer A, Dammerer D, Wansch J, Hackl W, Liebensteiner MC. Patella height correlates with trochlear dysplasia: a computed tomography image analysis. *Arthroscopy*. 2018;34(6):1921-1928.
32. Strecker W, Keppler P, Gebhard F, Kinzl L. Length and torsion of the lower limb. *J Bone Joint Surg Br*. 1997;79(6):1019-1023.
33. Weinberg DS, Liu RW. The association of tibia femur ratio and degenerative disease of the spine, hips, and knees. *J Pediatr Orthop*. 2017;37(5):317-322.
34. Dejour H, Walch G, Nove-Josserand L, Guier C. Factors of patellar instability: an anatomic radiographic study. *Knee Surg Sports Traumatol Arthrosc*. 1994;2(1):19-26.

SUPPORTING INFORMATION

Additional supporting information may be found online in the Supporting Information section.

How to cite this article: J Dan M, Parr WC, Crowley JD, et al. Moment arm function dictates patella sagittal height anatomy: Rabbit epiphysiodesis model alters limb length ratios and subsequent patellofemoral anatomical development. *J Orthop Res*. 2020;1–11.
https://doi.org/10.1002/jor.24714